

X-ray Diffraction, PGSE Diffusion, and Related NMR Studies on a Series of Cp*-Based Ru(IV)(Cp*)(η^3 -CH₂-CH-CHPh) Allyl Complexes

Ignacio Fernández and Paul S. Pregosin*

Laboratory of Inorganic Chemistry, ETH HCI, Hönggerberg CH-8093 Zürich, Switzerland

Alberto Albinati* and Silvia Rizzato

Department of Structural Chemistry (DCSSI), University of Milan, 20133 Milan, Italy

Received May 22, 2006

The new ruthenium (IV) allyl complexes [Ru(Cp*)Cl(DMF)(η^3 -CH₂-CH-CHPh)](PF₆) (**2b**) and [Ru(Cp*)Cl(t-BuCN)(η^3 -CH₂-CH-CHPh)](PF₆) (**2c**) have been prepared and their structures determined. These results are compared with the analogous X-ray data for [Ru(Cp*)Cl(CH₃CN)(η^3 -CH₂-CH-CHPh)](PF₆), [Ru(Cp*){OC(O-t-Bu)O}(η^3 -CH₂-CH-CHPh)](PF₆), [Ru(Cp*)(CH₃CN)₂(η^3 -CH₂-CH-CHPh)](PF₆)₂, and [Ru(Cp*)(DMF)₂(η^3 -CH₂-CH-CHPh)](PF₆)₂. In all of the structures, the Ru-(η^3 -CH₂-CH-CHPh) moiety is markedly distorted such that Ru-C(allyl) separation is much longer than the remaining two Ru-C(allyl) distances. The DMF and acetonitrile ligands are shown to exchange on the NMR time scale via both variable-temperature and 2-D exchange spectroscopy. Pulsed gradient spin-echo (PGSE) diffusion and ¹H,¹⁹F HOESY NMR methods show that there is relatively little ion pairing in these salts in DMF and acetonitrile solutions. The PF₆ anions take up specific positions with respect to the Ru(IV) cations.

Introduction

Ruthenium complexes have been described as useful catalysts in an increasing number of processes.¹ Ru-catalyzed allylic alkylation² and amination reactions,³ among others, have attracted significant interest due to the recognized regioselectivity in favor of branched products when starting from allylic precursors of the type R-CH=CH-CH₂-X (X = chloride, acetate, carbonate). The most commonly used catalyst precursor contains a Ru-Cp* fragment, e.g., [Ru(Cp*)(CH₃CN)₃](PF₆), **1**. Increasingly, a variety of derivatives of **1** are in use as catalysts, and these include chelating nitrogen ligands⁴ as well

as 1,5-COD⁵ complexes. In all these reactions, a ruthenium(IV) allyl complex is thought to be a common intermediate.

We have recently reported that, for the allylic alkylation reaction, the source of the observed branched-to-linear regioselectivity has an electronic origin.⁶ These conclusions were based on studies of two Ru(IV) allyl complexes: [Ru(Cp*)Cl(CH₃CN)(η^3 -CH₂-CH-CHPh)](PF₆), **2a**, and the carbonate complex [Ru(Cp*){OC(OBu^t)O}(η^3 -CH₂-CH-CHPh)](PF₆), **3**. We have subsequently prepared⁷ two new dicationic species, **4a,b**, and these and other complexes are shown in Scheme 1. Interestingly, while the monocations **2a** and **3** are useful in C-O,^{6c} C-N,^{6d} and C-C allylation reactions, via the use of oxygen, nitrogen, and carbon nucleophiles, respectively (see

(1) (a) Rigaut, S.; Touchard, D.; Dixneuf, P. H. *Coord. Chem. Rev.* **2004**, *248*, 1585–1601. (b) Haack, K. J.; Hashiguchi, S.; Fujii, A.; Ikariya, T.; Noyori, R. *Angew. Chem., Int. Ed. Engl.* **1997**, *36*, 285–288. (c) Hashiguchi, S.; Fujii, A.; Haack, K. J.; Matsumura, K.; Ikariya, T.; Noyori, R. *Angew. Chem., Int. Ed. Engl.* **1997**, *36*, 288–290. (d) Noyori, R. *Adv. Synth. Catal.* **2003**, *345*, 15–32. (e) Kondo, T.; Kodoi, K.; Nishinaga, E.; Okada, T.; Morisaki, Y.; Watanabe, Y.; Mitsudo, T. *J. Am. Chem. Soc.* **1998**, *120*, 5587–5588. (f) Grubbs, R. H. *Tetrahedron* **2004**, *60*, 7117–7140. (g) Trost, B. M.; Rudd, M. T. *J. Am. Chem. Soc.* **2005**, *127*, 4763–4776. (h) Ito, M.; Itahara, S.; Ikariya, T. *J. Am. Chem. Soc.* **2005**, *127*, 6172–6173. (i) Hejl, A.; Scherman, O. A.; Grubbs, R. H. *Macromolecules* **2005**, *38*, 7214–7218. (j) Drift, R. C.; Gagliardo, M.; Kooijman, H.; Spek, A. L.; Bouwman, E.; Drent, E. *J. Organomet. Chem.* **2005**, *690*, 1044–1055. (k) Kondo, T.; Mitsudo, T. *Chem. Lett.* **2005**, *34*, 1462–1467.

(2) (a) Trost, B. M.; Fraisse, P. L.; Ball, Z. T., *Angew. Chem., Int. Ed.* **2002**, *41*, 1059–1061. (b) Trost, B. M.; Crawley, M. L. *Chem. Rev.* **2003**, *103*, 2921–2943. (c) Mbaye, M. D.; Demerseman, B.; Renaud, J. L.; Toupet, L.; Bruneau, C. *Adv. Synth. Catal.* **2004**, *346*, 835–841.

(3) (a) Kondo, T.; Ono, H.; Satake, N.; Mitsudo, T.; Watanabe, Y. *Organometallics* **1995**, *14*, 1945–1953. (b) Cenini, S.; Ragaini, F.; Tollari, S.; Paone, D. *J. Am. Chem. Soc.* **1996**, *118*, 11964–11965. (c) Ragaini, F.; Cenini, S.; Tollari, S.; Tummolillo, G.; Beltrami, R. *Organometallics* **1999**, *18*, 928–942. (d) Matsushima, Y.; Onitsuka, K.; Kondo, T.; Mitsudo, T.; Takahashi, S. *J. Am. Chem. Soc.* **2001**, *123*, 10405–10406. (e) Takaya, J.; Hartwig, J. *J. Am. Chem. Soc.* **2005**, *127*, 5756–5757. (f) Mbaye, M. D.; Demerseman, B.; Renaud, J. L.; Bruneau, C. *J. Organomet. Chem.* **2005**, *690*, 2149–2158.

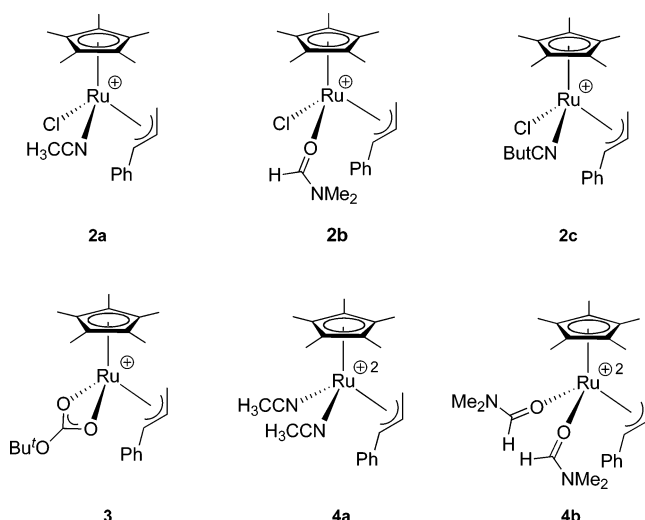
(4) (a) Kondo, H.; Kageyama, A.; Yamaguchi, Y.; Haga, M.; Kirchner, K.; Nagashima, H. *Bull. Chem. Soc. Jpn.* **2001**, *74*, 1927–1937. (b) Mbaye, M. D.; Demerseman, B.; Renaud, J. L.; Toupet, L.; Bruneau, C. *Angew. Chem. Int. Ed.* **2003**, *42*, 5066–5068. (c) Renaud, J. L.; Bruneau, C.; Demerseman, B. *Synlett* **2003**, 408–410. (d) Nagashima, H.; Kondo, H.; Hayashida, T.; Yamaguchi, Y.; Gondo, M.; Masuda, S.; Miyazaki, K.; Matsubara, K.; Kirchner, K. *Coord. Chem. Rev.* **2003**, *245*, 177–190. (g) Rubuz, N.; Ozdemir, I.; Cetinkaya, B.; Renaud, J. L.; Demerseman, B.; Bruneau, C. *Tetrahedron Lett.* **2006**, *47*, 535–538.

(5) (a) Zhang, S.; Mitsudo, T.; Kondo, T.; Watanabe, Y. *J. Organomet. Chem.* **1993**, *450*, 197–207. (b) Morisaki, Y.; Kondo, T.; Mitsudo, T. *Organometallics* **1999**, *18*, 4742–4746. (c) Kondo, T.; Morisaki, Y.; Uenoyama, S.; Wada, K.; Mitsudo, T. *J. Am. Chem. Soc.* **1999**, *121*, 8657–8658. (d) Shiotsuki, M.; Ura, Y.; Ito, T.; Wada, K.; Kondo, T.; Mitsudo, T. *J. Organomet. Chem.* **2004**, *689*, 3168–3172. (e) Tsujita, H.; Ura, Y.; Wada, K.; Kondo, T.; Mitsudo, T. *Chem. Commun.* **2005**, 5100–5102.

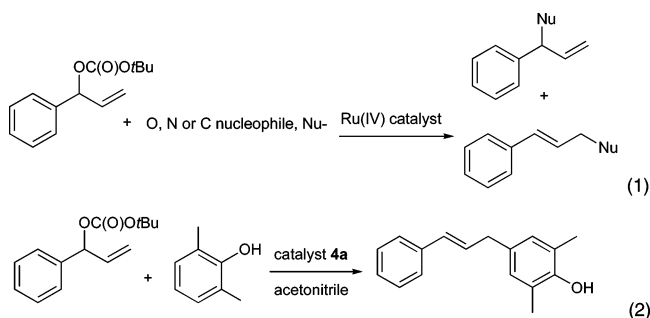
(6) (a) Hermatschweiler, R.; Fernández, I.; Pregosin, P. S.; Watson, E. J.; Albinati, A.; Rizzato, S.; Veiros, L. F.; Calhorda, M. J. *Organometallics* **2005**, *24*, 1809–1812. (b) Hermatschweiler, R.; Fernández, I.; Breher, F.; Pregosin, P. S.; Veiros, L. F.; Calhorda, M. J. *Angew. Chem., Int. Ed.* **2005**, *44*, 4397–4400. (c) Hermatschweiler, R.; Fernandez, I.; Pregosin, P. S.; Breher, F. *Organometallics* **2006**, *25*, 1440–1447. (d) Fernandez, I.; Hermatschweiler, R.; Pregosin, P. S.; Albinati, A.; Rizzato, S. *Organometallics* **2006**, *25*, 323–330.

(7) Fernández, I.; Hermatschweiler, R.; Breher, F.; Pregosin, P. S.; Veiros, L. F.; Calhorda, M. J. To appear in *Angew. Chem.*

Scheme 1



eq 1), the dication **4a**, in acetonitrile solution, affords a novel selective Friedel–Crafts catalyst,⁷ which gives *allylation of the phenyl ring* (e.g., eq 2).



We report here two new ruthenium(IV) allyl complexes, **2b,c**, and present X-ray crystallographic, diffusion, and NMR studies for a number of these and other salts. We are specifically seeking information with respect to (a) subtle structural distortions within the allyl ligand, (b) the structural influence of the solvent molecules acetonitrile and DMF, and (c) anion (PF₆)/cation interactions within these ruthenium(IV) allyl complexes. X-ray crystallography and NMR studies are ideally suited for the first two points. PGSE (pulse gradient spin–echo) NMR diffusion studies⁸ are now increasingly in use to recognize ion-pairing interactions in solution.^{9,10} When the PGSE studies are combined with ¹H,¹⁹F HOESY^{11,12} measurements, which describe the relative positions of the (fluorine-containing) anion, relative to the cation, one has a useful probe for point “c”, the question of ionic interactions. These various physical studies should provide

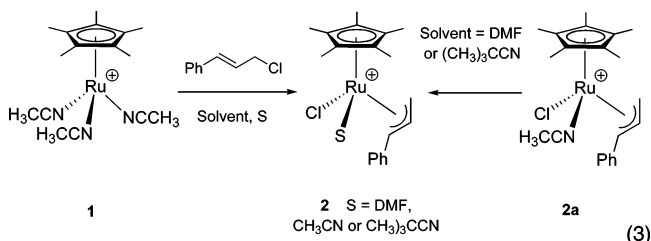
(8) (a) Stilbs, P. *Prog. NMR Spectrosc.* **1987**, *19*, 1. (b) Valentini, M.; Rügger, H.; Pregosin, P. S. *Helv. Chim. Acta* **2001**, *84*, 2833. (c) Antalek, B. *Concepts Magn. Reson.* **2002**, *14*, 225–258. (d) Pregosin, P. S.; Martinez-Viviente, E.; Kumar, P. G. A. *Dalton Trans.* **2003**, 4007. (e) Lucas, L. H.; Larive, C. K. *Concepts Magn. Reson.* **2004**, *20A*, 24–41. (f) Pregosin, P. S.; Kumar, P. G. A.; Fernández, I. *Chem. Rev.* **2005**, *105*, 2977. (g) Cohen, Y.; Avram, L.; Frish, L. *Angew. Chem., Int. Ed.* **2005**, *44*, 520–554. (h) Brand, T.; Cabrita, E. J.; Berger, S. *Prog. NMR Spectrosc.* **2005**, *46*, 159–196.

(9) (a) Valentini, M.; Pregosin, P. S.; Rügger, H. *Organometallics* **2000**, *19*, 2551. (b) Valentini, M.; Pregosin, P. S.; Rügger, H. *J. Chem. Soc., Dalton Trans.* **2000**, 4507. (c) Drago, D.; Pregosin, P. S.; Pfaltz, A. *Chem. Commun.* **2002**, 286. (d) Martínez-Viviente, E.; Rügger, H.; Pregosin, P. S.; López-Serrano, J. *Organometallics* **2002**, *21*, 5841. (e) Chen, Y.; Valentini, M.; Pregosin, P. S.; Albinati, A. *Inorg. Chim. Acta* **2002**, *327*, 4. (f) Kumar, P. G. A.; Pregosin, P. S.; Goicoechea, J. M.; Whittlesey, M. K. *Organometallics* **2003**, *22*, 2956.

a more comprehensive understanding of these salts and may mirror the source of their effectiveness in the differing catalytic reactions.

Results and Discussion

Preparation and Characterization. The complex Ru(IV) salts **2–4** have been prepared by oxidative addition reactions of either a chloro or carbonato substrate, in the appropriate solvent, e.g., see eq 3. One can also use an oxidative addition



approach to afford **2a** and then use a solvent exchange reaction, as indicated by the right-hand side of eq 3. All of these complex salts, see Scheme 1, have been characterized via NMR, mass spectral, and microanalytical studies, together with selected X-ray results. The complexes **2a** (80:20) and **2c** (82:18) reveal two isomers in solution; however, in other salts, e.g., **2b**, only one isomer is detected. We believe these two complexes are due to the presence of *endo* and *exo* isomers; that is, the central CH bond can point toward or away from the Cp* ligand, on the basis of 2-D NOESY measurements (see Figure 1). The Overhauser measurements show that the two terminal *anti*-allyl protons afford substantial NOE cross-peaks arising from the Cp* methyl groups, whereas an NOE to the central allyl proton resonance, from the Cp* methyl groups, is either absent or very weak. Further, one finds NOEs between the allyl phenyl protons and, for example, the DMF ligand, suggesting that these two are close in space and thus that the geometric isomer shown (DMF or acetonitrile proximate to the phenyl group) represents

(10) (a) Mo, H. P.; Pochapsky, T. C. *J. Phys. Chem. B* **1997**, *101*, 4485. (b) Beck, S.; Geyer, A.; Brintzinger, H. H. *Chem. Commun.* **1999**, 2477. (c) Jaing, Q.; Rügger, H.; Venanzi, L. M. *Inorg. Chim. Acta* **1999**, *290*, 64. (d) Zuccaccia, C.; Bellachioma, G.; Cardaci, G.; Macchioni, A. *Organometallics* **2000**, *19*, 4663. (e) Stoop, R. M.; Bachmann, S.; Valentini, M.; Mezzetti, A. *Organometallics* **2000**, *19*, 4117. (f) Burini, A.; Fackler, J. P.; Galassi, R.; Macchioni, A.; Omari, M. A.; Rawashdeh-Omari, M. A.; Pietroni, B. R.; Sabatini, S.; Zuccaccia, C. *J. Am. Chem. Soc.* **2002**, *124*, 4570. (g) Schlörer, N. E.; Cabrita, E. J.; Berger, S. *Angew. Chem., Int. Ed.* **2002**, *41*, 107. (h) Stahl, N. G.; Zuccaccia, C.; Jensen, T. R.; Marks, T. J. *J. Am. Chem. Soc.* **2003**, *125*, 5256.

(11) (a) Martínez-Viviente, E.; Pregosin, P. S. *Inorg. Chem.* **2003**, *42*, 2209. (b) Geldbach, T. J.; Breher, F.; Gramlich, V.; Kumar, P. G. A.; Pregosin, P. S. *Inorg. Chem.* **2004**, *43*, 1920. (c) Kumar, P. G. A.; Pregosin, P. S.; Schmid, T. M.; Consiglio, G. *Magn. Reson. Chem.* **2004**, *42*, 795–800. (d) Kumar, P. G. A.; Pregosin, P. S.; Bernardinelli, M. V. G.; Jazzar, R. F.; Viton, F.; Kündig, E. P. *Organometallics* **2004**, *23*, 5410–5418. (e) Schott, D.; Pregosin, P. S.; Jacques, B.; Chavarot, M.; Rose-Munch, F.; Rose, E. *Inorg. Chem.* **2005**, *44*, 5941–5948. (f) Schott, D.; Pregosin, P. S.; Veiros, L. F.; Calhorda, M. J. *Organometallics* **2005**, *24*, 5710–5717. (g) Fernández, I.; Pregosin, P. S. *Magn. Reson. Chem.* **2006**, *44*, 76–82.

(12) (a) Bellachioma, G.; Cardaci, G.; Macchioni, A.; Reichenbach, G.; Terenzi, S. *Organometallics* **1996**, *15*, 4349–4351. (b) Bellachioma, G.; Cardaci, G.; Gramlich, V.; Macchioni, A.; Valentini, M.; Zuccaccia, C. *Organometallics* **1998**, *17*, 5025–5030. (c) Bellachioma, G.; Cardaci, G.; D'Onofrio, F.; Macchioni, A.; Sabatini, S.; Zuccaccia, C. *Eur. J. Inorg. Chem.* **2001**, 1605–1611. (d) Romeo, R.; Fenech, L.; Scolaro, L. M.; Albinati, A.; Macchioni, A.; Zuccaccia, C. *Inorg. Chem.* **2001**, *40*, 3293–3302. (e) Zuccaccia, D.; Sabatini, S.; Bellachioma, G.; Cardaci, G.; Clot, E.; Macchioni, A. *Inorg. Chem.* **2003**, *42*, 5465. (f) Cavallo, L.; Macchioni, A.; Zuccaccia, C.; Zuccaccia, D.; Orabona, I.; Ruffo, F. *Organometallics* **2004**, *23*, 2137–2145. (g) Binotti, B.; Carfagna, C.; Foresti, E.; Macchioni, A.; Sabatino, P.; Zuccaccia, C.; Zuccaccia, D. *J. Organomet. Chem.* **2004**, *689*, 647–661.

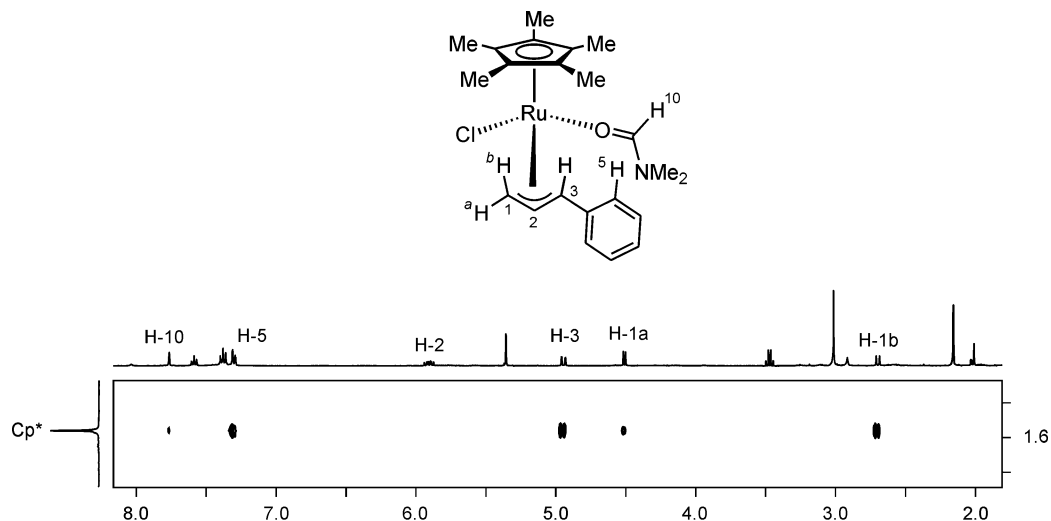


Figure 1. Section of the phase-sensitive $^1\text{H},^1\text{H}$ NOESY spectrum of **2b** at ambient temperature, showing the relatively strong contacts from the Cp* methyl groups to the terminal allyl *anti* protons H-1b and H-3. There is also a modest contact to the *syn* allyl proton H-1a and no contact to the central allyl proton. These data suggest that the *endo* configuration is the correct structure (CD_2Cl_2 , 500 MHz).

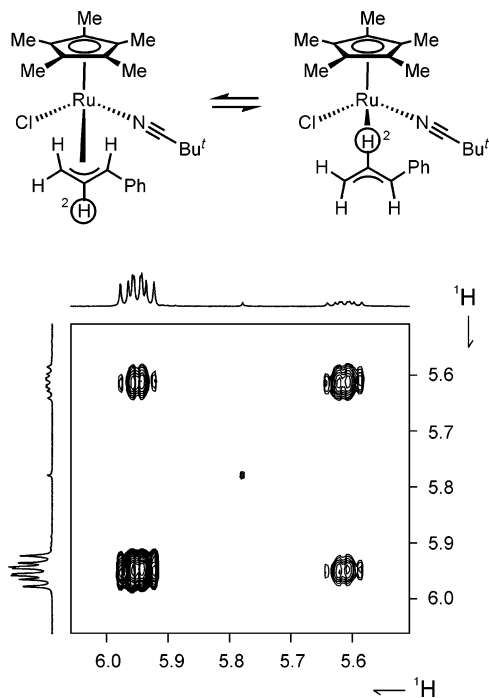
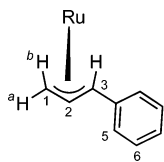


Figure 2. Section of the $^1\text{H},^1\text{H}$ phase-sensitive NOESY spectrum of **2c** at ambient temperature showing the exchange between the central allyl proton H-2 of the two isomers (CD_2Cl_2 , 500 MHz).

the correct structure. The two isomers observed are in exchange on the NMR time scale, as indicated by 2-D exchange spectroscopy (see Figure 2). Moreover, for **2b**, we observe exchange between the complexed DMF and traces of free DMF in solution. Table 1 gives selected ^1H and ^{13}C data for the major components in **2–4**. Exchange of Cl^- for either DMF or CH_3CN results in marked high-frequency shifts in all four allyl protons. We suggest that these changes are due to local anisotropic effects since (with one exception, see below) the appropriate allyl ^{13}C chemical shifts do not change markedly. Interestingly, the methylene allyl carbon resonance is found at much lower frequency than the terminal methine allyl carbon signal.

X-ray studies on $[\text{Ru}(\text{Cp}^*)\text{Cl}(\eta^3\text{-CH}_2\text{-CH-CHPh})(\text{DMF})](\text{PF}_6)$, **2b, and $[\text{Ru}(\text{Cp}^*)\text{Cl}(\eta^3\text{-CH}_2\text{-CH-CHPh})((\text{CH}_3)_3\text{CCN})](\text{PF}_6)$, **2c**.** Figures 3 and 4 show views of the Ru(IV) allyl cations. Selected bond distances and bond angles are given

Table 1. ^1H and ^{13}C NMR Allyl Chemical Shifts for the Ru(IV) Cp* Allyl Salts **2–4**



	H-1a	H-1b	H-2	H-3	H-5	C-1	C-2	C-3	C-5	C-7
2a^a	3.06	4.41	6.01	4.84	7.76	67.5	93.7	91.0	129.6	130.5
2b^b	2.68	4.51	5.91	4.94	7.31	64.4	95.9	92.3	129.4	130.7
2c^b	2.76	4.49	5.94	4.56	7.51	68.2	94.3	91.3	129.5	131.3
3^c	3.52	4.66	6.36	5.11	7.74	65.8	99.9	90.2	129.2	130.5
4a^a	3.41	4.87	6.59	5.31	7.90	66.3	94.1	103.3	129.9	130.5
4b^a	3.64	4.70	6.48	5.49	7.72	66.0	96.9	98.4	131.5	131.6

^a In $\text{Me}_2\text{CO}-d_6$. ^b In CD_2Cl_2 . ^c In $\text{DMF}-d_7$.

in Table 2. The immediate coordination sphere of the ruthenium cations contain a chloride donor, the $\eta^3\text{-CH}_2\text{-CH-CHPh}$ allyl ligand, the π -bound Cp*, and an oxygen-bound DMF molecule for **2b**, or a nitrogen bound *tert*-butylcarbonitrile molecule for **2c**. In both cations, the allyl ligand adopts the *endo* configuration with respect to the Cp*, as found in solution and in other published related examples.^{13b–e} The allyl C(Ph) terminal carbon is proximate to the coordinated solvent in both structures. Therefore, this structure corresponds to that of the major isomer in solution. The Ru to Cp* distances (centroid of the Cp ring) are 1.868(1) and 1.859(2) Å for **2b** and **2c**, respectively. The methyl groups of the Cp* are bent out of the plane defined by the five Cp* ring carbon atoms, away from the Ru atom. The PF_6 counterions in **2b,c** show short, nonbonding contacts in the range 2.5–2.6 Å (< van der Waals radii) to the H atoms of the Cp* methyl groups.

Whereas the Ru–Cl separations, 2.389 and 2.412 Å, and the Ru–O or Ru–N bond lengths, 2.113(2) and 2.068(2) Å, for

(13) (a) Orpen, A. G.; Brammer, L.; Allen, F. H.; Kennard, O.; Watson, D. G.; Taylor, R. *J. Chem. Soc., Dalton Trans.* **1989**, S1–S83. (b) Gemel, C.; Kalt, D.; Mereiter, K.; Sapunov, V. N.; Schmid, R.; Kirchner, K. *Organometallics* **1997**, *16*, 427–433. (c) Kondo, H.; Yamaguchi, Y.; Nagashima, H. *Chem. Commun.* **2000**, 1075–1076. (d) Hermatschweiler, R.; Fernández, I.; Breher, F.; Pregosin, P. S. *Organometallics* **2006**, *25*, 1440–1447. (e) A recent calculation supports this isomer as the more favored: Bi, S.; Ariaferd, A.; Jia, G.; Lin, Z. *Organometallics* **2005**, *24*, 680–686.

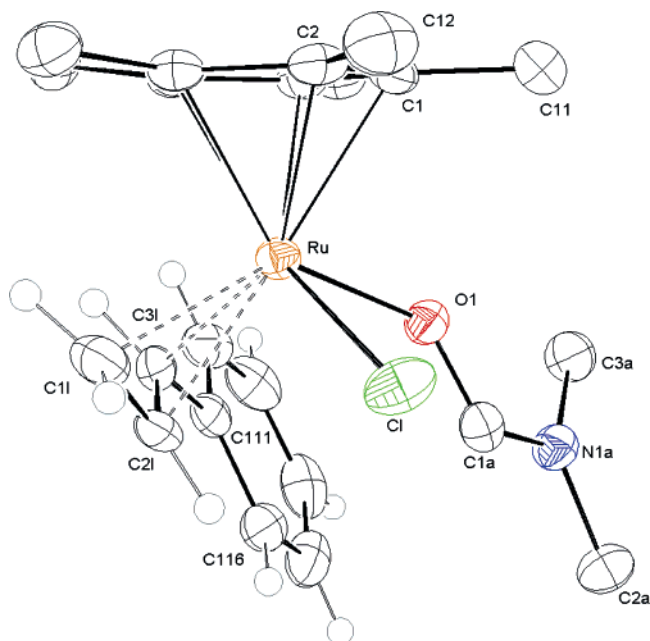


Figure 3. Structure of the cation $[\text{Ru}(\text{Cp}^*)\text{Cl}(\eta^3\text{-CH}_2\text{-CH-CHPh})(\text{DMF})]^+$ in **2b**. Thermal ellipsoids are drawn at 50% probability; PF_6^- anion is omitted for clarity.

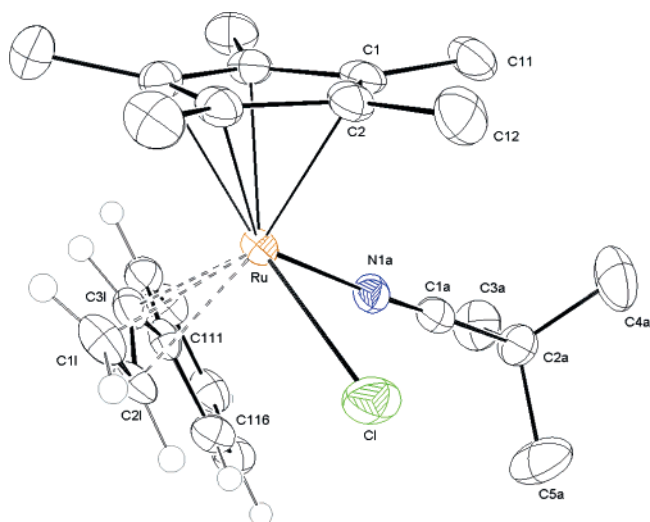


Figure 4. Structure of the cation $[\text{Ru}(\text{Cp}^*)\text{Cl}(\eta^3\text{-CH}_2\text{-CH-CHPh})(\text{CH}_3)_3\text{CCN}]^+$ in **2c**. Thermal ellipsoids are drawn at 50% probability; PF_6^- anion is omitted for clarity.

Table 2. Bond Lengths (Å) and Angles (deg) for 2b and 2c

	2b		2c
Ru–O(1)	2.113(2)	Ru–N(1A)	2.068(2)
Ru–Cl	2.3886(8)	Ru–Cl	2.4115(6)
Ru–C(1)	2.193(3)	Ru–C(1)	2.269(2)
Ru–C(2)	2.258(3)	Ru–C(2)	2.268(2)
Ru–C(3)	2.256(3)	Ru–C(3)	2.199(2)
Ru–C(4)	2.227(3)	Ru–C(4)	2.199(2)
Ru–C(5)	2.175(3)	Ru–C(5)	2.212(2)
Ru–C(1L)	2.164(4)	Ru–C(1L)	2.177(2)
Ru–C(2L)	2.157(3)	Ru–C(2L)	2.166(2)
Ru–C(3L)	2.320(3)	Ru–C(3L)	2.313(2)
O(1)–Ru–Cl	84.76(6)	N(1A)–Ru–Cl	81.69(6)

2b and **2c**, respectively, are as expected,^{13a} the three Ru–C(allyl) distances are worthy of note. For the two cations, the terminal allyl Ru–C bond lengths are markedly different. In the cation of **2b**, the Ru–C(allyl) distances are Ru(1)–C(1L), 2.164(4) Å, Ru(1)–C(2L), 2.157(3) Å, and Ru(1)–C(3L),

Scheme 2. Ruthenium–Carbon Allyl Bond Distances (Å), in the Various Salts, 2 to 4

Structure	Ru–C(1L)	Ru–C(2L)	Ru–C(3L)
2a	2.192	2.162	2.351
2b	2.164	2.157	2.320
2c	2.177	2.166	2.313
3	2.162	2.137	2.303
4a	2.180	2.189	2.382
4b	2.184	2.155	2.323

2.320(3) Å. In the cation of **2c**, the distances are Ru(1)–C(1L), 2.177(2) Å, Ru(1)–C(2L), 2.166(2) Å, and Ru(1)–C(3L), 2.313(2) Å. Obviously, the separations from the two terminal allyl carbons, C(1) and C(3), are different by ca. 0.13–0.15 Å, suggesting very different bond strengths to these carbon atoms. This conclusion is also supported by the observed ¹³C data given in Table 1. In a recent structural report^{2c} Bruneau and co-workers find for $\text{Ru}(\text{CH}_3\text{CN})(\eta^3\text{-CH}_2\text{-CH-CH}_2)(\text{Br})\text{Cp}^*$ Ru–C bond lengths of 2.280(5), 2.165(5), and 2.208(4) Å, with the largest value for the RuCH(CH₃) distance and the smallest for the central allyl carbon. Although not quite so marked, once again the value for the substituted allyl carbon is consistent with the observed trend.

Scheme 2 shows a comparison of the Ru–C allyl bond lengths for all of our Cp* $\text{Ru}(\eta^3\text{-PhCH-CH-CH}_2)$ cationic derivatives. All of the structures reveal strongly asymmetrically bound allyl moieties, with the bis-acetonitrile cation having the largest Ru–C3 bond length, ca. 2.38 Å. The substitution of a chloride by a DMF molecule, i.e., going from **2b** to **4b**, does not affect the Ru–C3 bond distance; however, substituting chloride by acetonitrile (**2a** to **4a**) significantly affects the Ru–C3 bond length.

During an earlier preparation of the neutral Ru(IV) Cp allyl complex $\text{RuCpCl}_2(\eta^3\text{-CH}_2\text{-CH-CH}_2)$ a small amount of a crystalline material precipitated from acetone solution (see Experimental Section). The solid-state structure of this material was determined and found to be the dinuclear Ru(III) species $[\text{Ru}(\text{Cp})\text{Cl}(\mu\text{-Cl})_2]_2$, **5**. A view of this molecule is shown in Figure 5, and selected bond lengths and bond angles are given in the caption.

The five Ru–C(Cp) separations in **5**, and in **2b,c** as well (see Table 2), are clearly significantly different, although there seems no obvious reason for this in these three structures. We also note that, in the Cp* rings, the C–C bond distances are not equivalent, showing a trend that associates the shortest

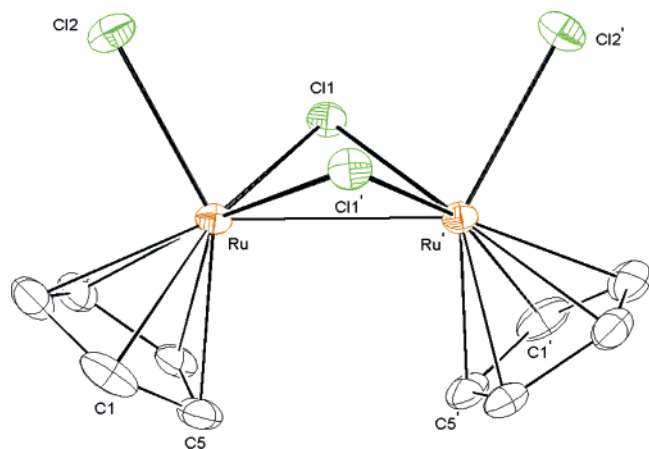


Figure 5. Dinuclear Ru(III) Cp complex **5**. Ru–Ru = 2.7748(6) Å, Ru–Cl(1) = 2.3591(8) Å, Ru–Cl(1') = 2.3788(8) Å, Ru–Cl(2) = 2.3851(8) Å, Ru–C(1) = 2.229(3) Å, Ru–C(2) = 2.207(3) Å, Ru–C(3) = 2.167(3) Å, Ru–C(4) = 2.156(3) Å, Ru–C(5) = 2.195(3) Å, Cl(1)–Ru–Cl(2) = 87.87(3)°, Ru–Cl(1)–Ru' = 71.70(2)°.

separations with the longest Ru–C distances. This observation is consistent with a subtle interplay of electronic and steric factors associated with the change in the ligands.

The Ru to Cp distance (to the centroid of the Cp ring in **5**), at 1.830(3) Å, is somewhat shorter than that measured for **2b,c** (1.859(2) and 1.861(1) Å, respectively). This difference is likely due to the differing steric effects associated with Cp* relative to Cp. We presume that complex **5** is formed via a slow radical process involving loss of the allyl ligand. Complex **5** is worthy of note in that allyl chloride derivatives are occasionally used in organic allylation chemistry.

Solution NMR Studies. Since the bis-DMF salt, **4b**, was used as a catalyst precursor, in acetonitrile solution, it was of interest to monitor the rate of DMF/acetonitrile exchange. Figure 6 shows the curve derived from ¹H NMR data for this exchange process (using the appearance of free DMF as a monitor), at room temperature in CD₃CN solution. Surprisingly, after 1 h at probe ambient temperature, only 84% of the DMF had

exchanged despite the large excess of nitrile. This suggests a relatively slow dissociation of DMF from the 18e Ru(IV) dication. However, at 353 K, the temperature at which the Friedel–Crafts C–C bond making catalysis is run (eq 2), the exchange of the two DMF solvent molecules took place within 1 min. This supports the validity of assuming that **4a** is indeed the relevant catalyst precursor.

The crystallographic data for **2b**, **2c**, and **5** hinted at some differences in the Ru–C(Cp*) separations. Consequently, variable-temperature NMR measurements were performed for complex **2b** in the range 298–155 K, and these are shown in Figure 7. The rotation of the Cp* is still rapid at 155 K since we find no significant broadening of the Cp* methyl resonance; however, the rotation of the allyl phenyl ring about the C(*ipso*)–C(Ph) bond is now restricted on the NMR time scale at ca. 163 K. The nonequivalent resonances for two *ortho* and *meta* protons are clearly visible. Further, one of the two nonequivalent DMF methyl groups experiences a low-frequency shift ($\Delta\delta = -0.2$ ppm), and we assign this to an anisotropic effect due to the proximate allyl phenyl group. Consequently, the source of the difference in the Ru–C separations, observed from the X-ray data, remains unclear.

Diffusion NMR and HOESY Studies. It seemed likely that a comparison of mono- vs dicationic salts might reveal differences in how the PF₆ anions interact with the organometallic cations. As in previous studies, we measure the experimental diffusion constants (*D*-values) via pulsed gradient spin-echo (PGSE) methods and then calculate the corresponding hydrodynamic radii, *r*_H, via the Stokes–Einstein equation (eq 4).

$$r_H = kT/6\pi\eta D \quad (4)$$

D = diffusion constant and η = viscosity

It is assumed that, when a relatively large cation and a relatively small anion reveal similar *D*-values, this indicates substantial ion pairing. The use of the constant “6” in eq 4 has been criticized,¹⁴ so that in Table 3 we show both conventional (using 6) and corrected, *r*, constants. The factor *c* can vary from 4

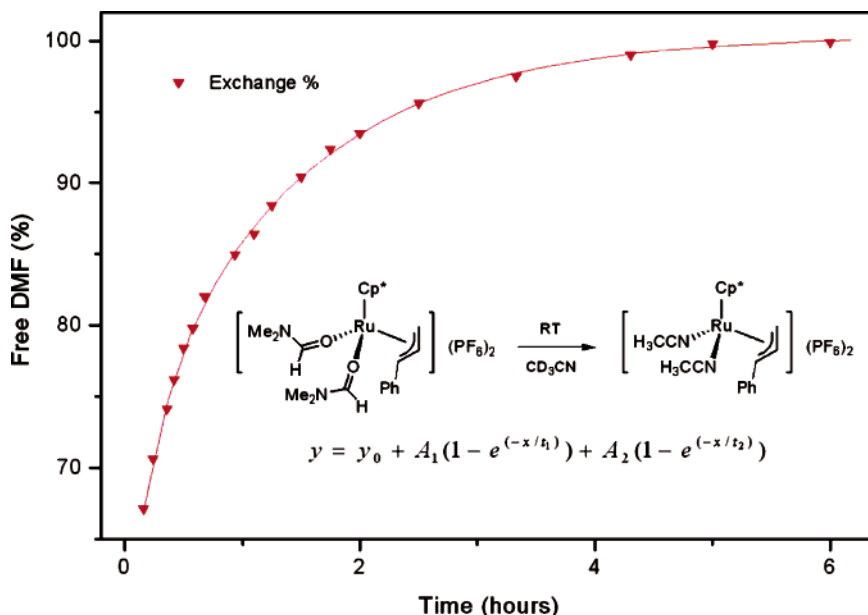


Figure 6. Solvent exchange of the bis-DMF complex [RuCp*(η^3 -CH₂-CH-CHPh)(DMF)₂](PF₆)₂, **4b**, to afford the bis-acetonitrile complex [RuCp*(η^3 -CH₂-CH-CHPh)(CH₃CN)₂](PF₆)₂, **4a**. Salt **4b** was dissolved in CD₃CN, and the appearance of free DMF was monitored by ¹H NMR spectroscopy ($y_0 = 57.16157$; $A_1 = 13.68922$; $t_1 = 0.2404$; $A_2 = 29.50985$; $t_2 = 1.37759$).

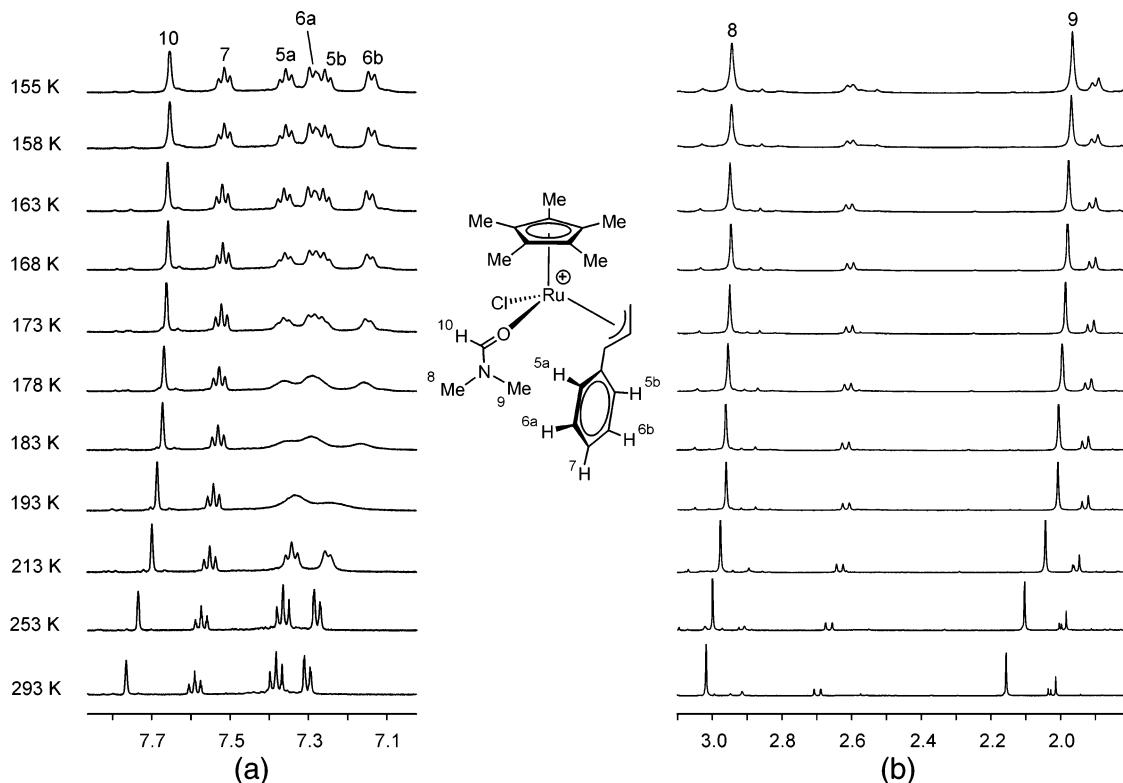


Figure 7. Variable-temperature ¹H NMR spectra for a sample of **2b**. The change in the aromatic region (a) stems from the restricted rotation around the C(*ipso*)-C(Ph) bond, whereas the pronounced low-frequency shift of one of the DMF methyl groups (b) is assigned to an anisotropic effect (500 MHz, CD₂Cl₂).

(slip boundary conditions¹⁴) to 6 (stick boundary conditions¹⁴) and stems from semiempirical estimations derived from the microfriction theory proposed by Wirtz and co-workers,¹⁴ in which *c* is expressed as a function of the solute-to-solute ratio of radii. For the 2 mM measurements, the table gives three *r_H* values: using *c* = 6, a corrected *c*, and an *r_x* estimated using the program Chem3D.

The table shows *D*-values for 2 mM acetonitrile or DMF samples of **2a**, **2b**, **4a**, and **4b** (and then a set of data at higher concentrations for **4a** and **4b**). From the measured *D*-value, for the chloro-DMF cation of **2b**, in DMF solution, we estimate the hydrodynamic radius, *r_H*, to be ca. 4.9 Å, in good agreement with estimates of the size of this cation, 4.6 Å, from our crystallographic data. For the 2 mM result from the bis-DMF cation, **4b**, we obtain an *r_H* value of ca. 5.7 Å, a much larger value. The *D*-value for the bis-nitrile dication, **4a**, in acetonitrile solution, is also somewhat large at 5.4 Å.

Ion pairing can result in markedly increased *r_H* values; however, the diffusion data for the PF₆ anions from the 2 mM solutions of **2a**, **2b**, **4a**, and **4b** suggest that this is not the case. The 2.2–2.8 Å *r_H* values for these PF₆ anions are suggestive of well-separated ions and typical of what one finds in polar solvents of high dielectric constant. The *r_H* values for the PF₆ anions in DMF solution are even somewhat smaller than those normally found in methanol solution.⁹

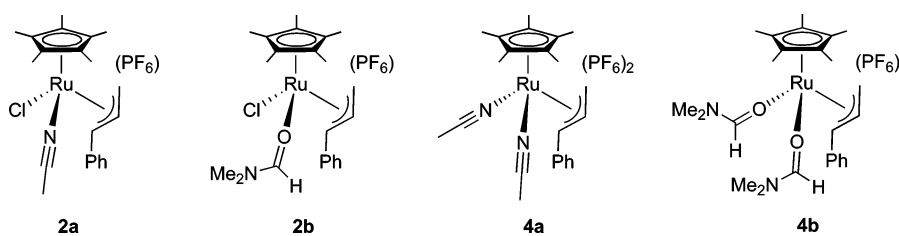
(14) (a) It has been suggested that the factor *c* (= 6 in eq 4) is not valid for small species whose van der Waals radii are <5 Å (Edward, J. T. *J. Chem. Educ.* **1970**, *47*, 261). This factor can be adjusted by using a semiempirical approach (see: Chen, H.-C.; Chen, S.-H. *J. Phys. Chem.* **1984**, *88*, 5118; Espinosa, P. J.; de la Torre, J. G. *J. Phys. Chem.* **1987**, *91*, 3612) derived from the microfriction theory proposed by Wirtz and co-workers (Gierer, A.; Wirtz, K. *Z. Naturforsch., A* **1953**, *8*, 522; Spernl, A.; Wirtz, K. *Z. Naturforsch., A* **1953**, *8*, 532). (b) Zuccaccia, D.; Macchioni, A. *Organometallics* **2005**, *24*, 3476–3486.

Possibly, the larger *r_H* values for the dications arise due to some charge-induced aggregation; that is, the 2+ charge on the cation could increase the tendency toward aggregation. To test this idea, we have measured the *D*-values for **4a** and **4b** at both 10 and 20 mM. The observed concentration dependence for the bis-DMF dication is small. Indeed, there is no difference between the 2 and 10 mM solutions. However, for the bis-nitrile dication, **4a**, the *D*-values decrease 2–3% (and thus the *r_H* values increase) with each increase in concentration. It seems likely that for the bis-nitrile salt **4a** we are dealing with some aggregation as a function of concentration. Aggregation at higher concentrations is now fairly well known.^{15,16} Different aggregation states or different ratios of aggregates might affect the reactivity.

¹H,¹⁹F HOESY spectroscopy is often helpful in positioning the anions in three-dimensional space, relative to the cations. Figure 8 shows ¹H,¹⁹F HOESY spectra for **2a**, **3**, and **4a**. The figure shows that, for the monocation **2a**, the anion approaches only the Cp* methyl groups. The situation is similar for the monocationic carbonate, **3**, although there is a weak contact to the *t*-Bu methyl groups. However in the bis-nitrile dication, **4a**, in addition to the Cp* methyl interaction, there are now well-

(15) (a) Zuccaccia, D.; Clot, E.; Macchioni, A. *New J. Chem.* **2005**, *29*, 430–433. Macchioni, A.; Romani, A.; Zuccaccia, C.; Guglielmetti, G.; Querci, C. *Organometallics* **2003**, *22*, 1526–1533 (b) Song, F. Q.; Lancaster, S. J.; Cannon, R. D.; Schormann, M.; Humphrey, S. M.; Zuccaccia, C.; Macchioni, A.; Bochmann, M. *Organometallics* **2005**, *24*, 1315–1328. (c) We have not measured the solution viscosities. However, we have measured, and show in Table 3, the *D*-values for the solvents, acetonitrile and DMF, for the three concentrations. These values are not very different and, allowing for an error of “6” in the last figure, do not support a significant change in the viscosities of these solutions.

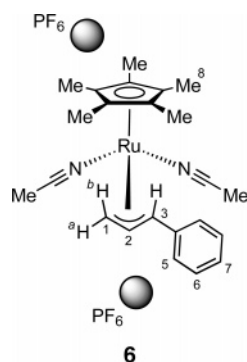
(16) Using our data, a reviewer has calculated that **4a,b** exist as “ion triples” containing two cations and one anion. Further, he suggests some aggregation for **2a,b**.

Table 3. D and r_H (Å) Values for the Ru Complexes **2a,b** and **4a,b** in Acetonitrile and DMF Solutions


	C (mM)	solvent	nucleus	D^a	r_H^b	r_X^c	c	r^d
2a	2	CH ₃ CN	¹ H	13.72	4.7	4.5	5.6	5.1
			¹⁹ F	24.76	2.6	1.6	4.7	3.3
2b	2	DMF	¹ H (CH ₃ CN)	40.34	1.6			
			¹ H	5.20	4.9	4.6	5.5	5.4
			¹⁹ F	11.40	2.2	1.6	3.8	3.5
			¹ H (DMF)	14.04	1.8			
4a	2	CH ₃ CN	¹ H	12.07	5.4	4.6	5.7	5.7
			¹⁹ F	23.50	2.8	1.6	4.9	3.4
			¹ H (CH ₃ CN)	40.35	1.6			
			¹ H	11.82	5.5			
4a	10	CH ₃ CN	¹⁹ F	22.69	2.9			
			¹ H (CH ₃ CN)	40.40	1.6			
			¹ H	11.49	5.6			
			¹⁹ F	21.57	3.0			
4a	20	CH ₃ CN	¹ H	14.51	1.8			
			¹ H (CH ₃ CN)	40.28	1.6			
			¹ H	4.44	5.7	4.8	5.6	6.2
			¹⁹ F	11.05	2.3	1.6	4.0	3.5
4b	2	DMF	¹ H (DMF)	14.48	1.8			
			¹ H	4.45	5.7			
			¹⁹ F	10.59	2.4			
			¹ H (DMF)	14.56	1.8			
4b	10	DMF	¹ H	4.37	5.8			
			¹⁹ F	10.19	2.5			
			¹ H (DMF)	14.51	1.8			
			¹⁹ F	10.19	2.5			

^a $\times 10^{-10} \text{ m}^2 \text{ s}^{-1}$, 299 K, at 2 mM. $\pm 2\%$. ^b The viscosity, η , used in the Stokes–Einstein equation is (DMF, 299 K) = 0.8574×10^{-3} ; (CH₃CN, 299 K) = 0.3377. The value “6” was used. ^c Estimated using Chem3D, by averaging the distances between the centroid and the outer hydrogen. ^d Using the “c” value shown immediately to the right.

resolved ¹H, ¹⁹F contacts from the PF₆ to the *central* allyl proton H-2 and the *ortho* phenyl protons H-5.¹⁶ The Overhauser contacts in **4a** may well result from the necessity of placing two anions in three-dimensional space such that the anion–anion repulsion is minimal. To this end, we suggest a structure such as **6** as a partial contributor to the overall solution structure. The anions lie above and below the cation and thus explain the



observed contact to the central allyl proton, H-2. The presence of one of the two anions in the region of the allyl ligand (in addition to some aggregation) might well have steric consequences with respect to an incoming phenol nucleophile.

Comments. The physical studies reveal that these Ru(IV) allyl complexes all have markedly distorted allyl ligands, both in the solid and in the solution states. At room temperature the dimethyl formamide Ru complex, **4b**, slowly exchanges the

complexed DMF ligands for solvent CH₃CN. However, the exchange is rapid at elevated temperature. The resulting Ru(IV) bis-acetonitrile species, **4a**, which performs Friedel–Crafts type allylation chemistry, rather than simple O-, N-, or C-allylation, (a) possesses the longest Ru–C3 bond length, (b) may aggregate in acetonitrile solution, and (c) has one of the two PF₆ anions fairly close to the complexed η^3 -CH₂–CH–CHPh allyl ligand. The diffusion data clearly show that the anion does not reside permanently in this position. Nevertheless, this position of the anion, plus some aggregation, might result in sufficient steric hindrance such that aromatic allylation would be preferred to the more routine attack of the nucleophile at allyl carbon C3.

Experimental Part

All reactions and manipulations were performed under a N₂ atmosphere using standard Schlenk techniques. Solvents were dried and distilled under standard procedures and stored under nitrogen. All the standard one- and two-dimensional measurements were performed on Bruker Avance 300, 400, and 500 MHz spectrometers using samples of 2–20 mM concentration. Chemical shifts are given in ppm and referenced to TMS and CFCl₃ for ¹H and ¹⁹F, respectively. Elemental analyses and mass spectroscopic studies were performed at ETHZ.

Crystallography. Red crystals of [Ru(Cp*)Cl(Me₂NCHO)(η^3 -CH₂–CH–CHPh)](PF₆) (**2b**) and [Ru(Cp*)Cl[(CH₃)₃CCN](η^3 -CH₂–CH–CHPh)](PF₆) (**2c**), suitable for X-ray diffraction, were obtained by layering diethyl ether in a CH₂Cl₂ solution of the

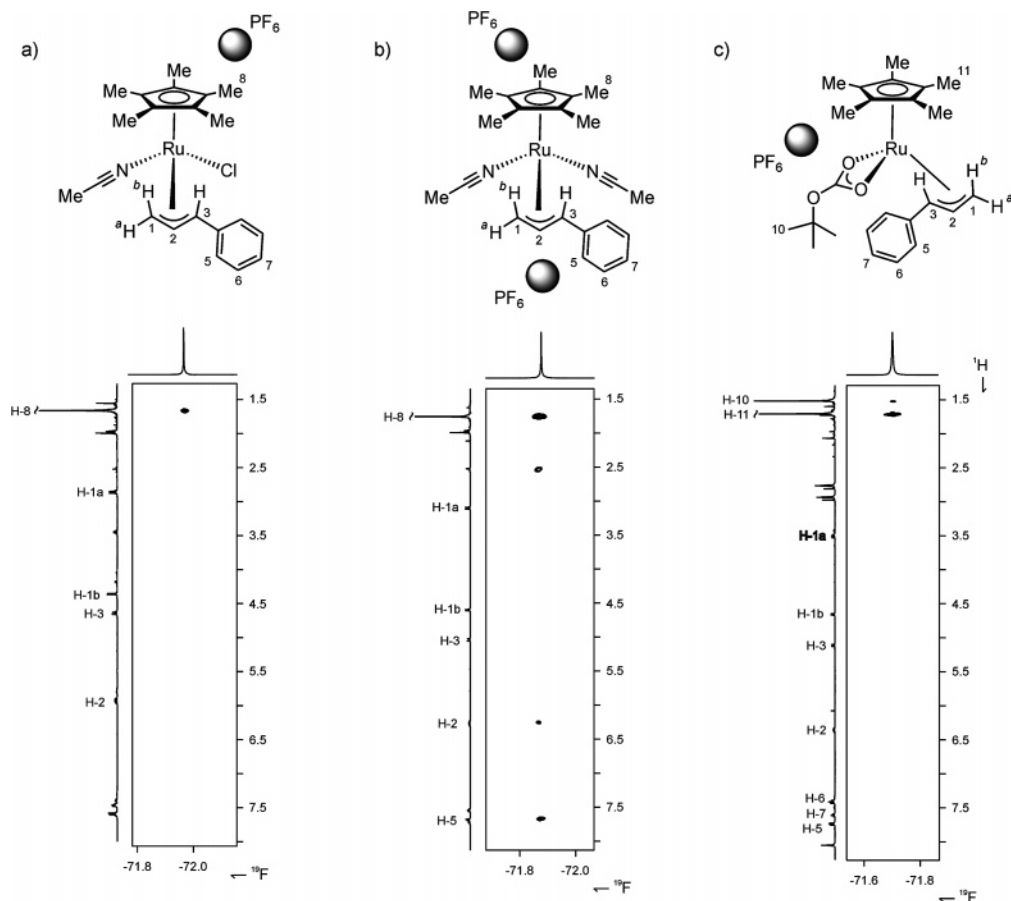


Figure 8. ^{19}F , ^1H HOESY spectra of 10 mM samples at ambient temperature of (a) $[\text{Ru}(\text{Cp}^*)\text{Cl}(\text{CH}_3\text{CN})(\eta^3\text{-CH}_2\text{-CH-CHPh})](\text{PF}_6)$, **2a**, in CD_3CN ; (b) $[\text{Ru}(\text{Cp}^*)(\text{CH}_3\text{CN})_2(\eta^3\text{-CH}_2\text{-CH-CHPh})](\text{PF}_6)$, **4a**, in CD_3CN ; and (c) $[\text{Ru}(\text{Cp}^*)(\text{OCO}_2t\text{Bu})(\eta^3\text{-CH}_2\text{-CH-CHPh})](\text{PF}_6)$, **3**, in DMF. In the fluorine dimension only one of the two resonances of the doublet is shown. For **4a**, the cross-peak at ca. 2.5 ppm stems from those acetonitrile ligands, which have not yet exchanged with the deuterioacetonitrile (^1H , 400 MHz).

isolated complex and are air-stable. Red, plate-like, crystals of $[\text{Ru}(\text{Cp})\text{Cl}_2]_2$ were obtained from acetone solution. The crystals were mounted on Bruker diffractometers, equipped with CCD detectors, for the unit cell and space group determinations. The crystals for the data collection were cooled to 120 K (110 K for **2c**) using a cold nitrogen stream. Selected crystallographic and other relevant data are listed in Table 4 and in the Supporting Information.

Data were corrected for Lorentz and polarization factors with the data reduction software SAINT¹⁷ and corrected empirically for absorption using the SADABS program.¹⁸ The structures were solved by Patterson and Fourier methods and refined by full matrix least-squares¹⁹ (the function minimized being $\sum[w(F_o - 1/kF_c)^2]$). For all the structures, no extinction correction was deemed necessary. The scattering factors used, corrected for the real and imaginary parts of the anomalous dispersion, were taken from the literature.²⁰ All calculations were carried out by using the PC version of SHELX-97¹⁹ and ORTEP programs.²¹

Structural Study of $[\text{Ru}(\text{Cp}^*)\text{Cl}(\text{Me}_2\text{NCHO})(\eta^3\text{-CH}_2\text{-CH-CHPh})]\text{PF}_6$ (2b**).** The space group was unambiguously determined from the systematic absences, while the cell constants (at 120 K) were refined by least-squares, at the end of the data collection, using

(17) BrukerAXS, SAINT, Integration Software; Bruker Analytical X-ray Systems: Madison, WI, 1995.

(18) Sheldrick, G. M. SADABS, Program for Absorption Correction; University of Göttingen: Göttingen, Germany, 1996.

(19) Sheldrick, G. M. SHELX-97, Structure Solution and Refinement Package; Universität Göttingen, 1997.

(20) International Tables for X-ray Crystallography; Wilson, A. J. C., Ed.; Kluwer Academic Publishers: Dordrecht, The Netherlands, 1992; Vol. C.

(21) Farrugia, L. J. J. Appl. Crystallogr. 1997, 30, 565.

3622 reflections ($\theta_{\text{max}} \leq 24.3^\circ$). The data were collected by using ω scans, in steps of 0.3° . For each of the 1515 collected frames, counting time was 30 s. The least-squares refinement was carried out using anisotropic displacement parameters for all non-hydrogen atoms. The H atoms of the allylic moiety were found from difference Fourier maps and refined using isotropic temperature factors, while the contribution of the remaining hydrogens, in their calculated positions ($\text{C-H} = 0.96$ (Å), $B(\text{H}) = 1.2B(\text{C}_{\text{bonded}})$ (Å²), was included in the refinement using a riding model.

Structural Study of $[\text{Ru}(\text{Cp}^*)\text{Cl}[(\text{CH}_3)_3\text{CCN}](\eta^3\text{-CH}_2\text{-CH-CHPh})](\text{PF}_6)$ (2c**).** The space group was determined from the systematic absences, while the low-temperature cell constants were refined by least-squares, at the end of the data collection, using 9821 reflections ($\theta_{\text{max}} \leq 25.5^\circ$). The data were collected by using ω scans, in steps of 0.3° . For each of the 1800 collected frames, counting time was 30 s. The least-squares refinement was carried out using anisotropic displacement parameters for all non-hydrogen atoms, while the H atoms were included in the refinement as described above. The PF_6^- anion showed positional disorder for several equatorial fluorine atoms. Two different orientations for the F atoms were clearly shown in the difference Fourier maps; the resulting disordered model was refined anisotropically (sof's 0.66 and 0.34, respectively).

Structural Study of $[\text{Ru}(\text{Cp}^*)\text{Cl}_2]_2$ (5**).** Space group and cell constants were determined at 120 K. The values of the cell parameters were refined at the end of the data collection using 1012 reflections ($\theta_{\text{max}} \leq 22.5^\circ$). The data were collected by using ω scans, in steps of 0.3° . For each of the 1860 collected frames, counting time was 30 s. The least-squares refinement was carried out using

Table 4. Experimental Data for the X-ray Study of **2b**, **2c**, and [RuCPCl₂]₂

	2b	2c	[RuCPCl ₂] ₂
formula	C ₂₂ H ₃₁ ClF ₆ NOPRu	C ₂₄ H ₃₃ ClF ₆ NPRu	C ₁₀ H ₁₀ Cl ₄ Ru ₂
mol wt	606.97	617.00	474.12
data coll. T, K	120 (2)	110 (2)	120(2)
diffractometer	Bruker APEX	Bruker APEX	Bruker SMART
cryst syst	monoclinic	monoclinic	monoclinic
space group (no.)	<i>P</i> 2 ₁ / <i>c</i> (14)	<i>P</i> 2 ₁ / <i>n</i> (14)	<i>C</i> 2/ <i>c</i> (15)
<i>a</i> , Å	8.2667(6)	8.4912(4)	6.988(2)
<i>b</i> , Å	17.441(1)	14.6540(6)	12.489(3)
<i>c</i> , Å	17.372(1)	21.1911(9)	14.649(3)
β, deg	101.083(2)	97.822(1)	99.121(5)
<i>V</i> , Å ³	2458.0(3)	2612.3(2)	1262.3(5)
<i>Z</i>	4	4	4
ρ _{calcd} , g cm ⁻³	1.640	1.569	2.495
μ, cm ⁻¹	8.72	8.20	32.05
radiation		Mo Kα (graphite monochrom., λ = 0.71073 Å)	
θ range, deg	1.67 < θ < 26.62	1.69 < θ < 26.03	2.82 < θ < 25.01
no. data collected	19 469	18 232	5262
no. indep data	5120	5144	1106
no. obsd reflns (<i>n</i> _o)	4163	4692	1012
[<i>F</i> _o ² > 2.0σ(<i>F</i> ²)]			
no. of params refined (<i>n</i> _v)	326	388	73
<i>R</i> _{int}	0.0475	0.0287	0.0287
<i>R</i> (obsd reflns) ^a	0.0399	0.0312	0.0175
<i>R</i> _w ² (obsd reflns) ^b	0.0926	0.0818	0.0201
GOF ^c	1.026	1.049	1.016

^a $R = \sum(|F_o - (1/k)F_c|)/\sum|F_o|$. ^b $R_w^2 = [\sum w(F_o^2 - (1/k)F_c^2)^2/\sum w|F_o|^2]$. ^c $GOF = [\sum w(F_o^2 - (1/k)F_c^2)^2/(n_o - n_v)]^{1/2}$.

anisotropic displacement parameters for all non-hydrogen atoms. The contribution of the hydrogen atoms, in their calculated positions ($C-H = 0.96(\text{Å})$, $B(H) = 1.2B(C_{\text{bonded}})(\text{Å}^2)$), was included in the refinement using a riding model.

Diffusion NMR. All the diffusion measurements were performed on a 400 MHz Bruker Avance spectrometer equipped with a microprocessor-controlled gradient unit and an inverse multinuclear probe with an actively shielded Z-gradient coil. The shape of the gradient pulse was rectangular, and its strength varied automatically in the course of the experiments. The measurements were carried out without spinning. The sample temperature was calibrated, before the PGSE measurements, by introducing a thermocouple inside the bore of the magnet. The calibration of the gradients was carried out via a diffusion measurement of H₂O in D₂O, which afforded a slope of 2.022×10^{-4} . We estimate the experimental error in the *D*-values to be $\pm 2\%$. All of the data leading to the reported *D*-values afforded lines whose correlation coefficients were > 0.999 , and 8–12 points have been used for regression analysis. To check reproducibility, three different measurements with different diffusion parameters (δ and/or Δ) were always carried out. The gradient strength was incremented in 8% steps from 10% to 98%. A measurement of ¹H and ¹⁹F *T*₁ was carried out before each diffusion experiment, and the recovery delay set to 5 times *T*₁.

In the ¹H-PGSE experiments δ was set to 2 ms. The number of scans varied between 80 and 128 per increment with a recovery delay of 5 to 10 s. Typical experimental times were 4–5 h.

For ¹⁹F, δ was usually set from 1.5 to 3 ms. Eight to 16 scans were taken with a recovery delay of 10 to 20 s, and a total experimental time of ca. 2–4 h.

The ¹H,¹H NOESY spectra were acquired using a 1 s relaxation delay and 800 ms of mixing time. The ¹⁹F,¹H HOESY measurements were carried out with a doubly tuned (¹H, ¹⁹F) TXI probe. A mixing time of 800 ms was used, and 32–64 scans were taken for each of the 512 *t*₁ increments recorded. The delay between increments was set to 2 s.

[RuCp*Cl(Me₂NCHO)(η³-CH₂-CH-CHPh)]PF₆ (**2b**). Dimethylformamide (2 mL) was added to an oven-dried Schlenk containing [RuCp*Cl(CH₃CN)(η³-CH₂-CH-CHPh)](PF₆), **2a** (100 mg, 0.174 mmol). The reaction mixture was stirred for 2 h, after which the solution was slowly concentrated under vacuum. The resulting crude was washed with CH₂Cl₂/diethyl ether, affording

a red solid, which was filtrated and dried under vacuum, 102 mg (88%). A dichloromethane solution of this solid was then layered with diethyl ether and stored at -30 °C during 24 h, affording crystals of **2b**, suitable for X-ray diffraction. ¹H NMR (CD₂Cl₂, 298 K, 400 MHz): δ 1.58 (15H), 2.15 (3H, *J* 0.8 Hz), 2.68 (1H, *J* 9.6 Hz), 3.01 (3H), 4.51 (1H, *J* 6.4 Hz), 4.94 (1H, *J* 11.2 Hz), 5.91 (1H, *J* 11.2, 9.6, 6.4 Hz), 7.30 (2H, *J* 8.4, 1.2 Hz), 7.38 (2H, *J* 8.4, 7.6 Hz), 7.58 (1H, *J* 7.6, 1.2 Hz), 7.76 (1H). ¹³C NMR (CD₂-Cl₂, 298 K, 400 MHz): δ 9.6 (CH₃), 33.2 (CH₃), 39.6 (CH₃), 64.4 (H₂C_{allyl}), 92.3 (HC_{allyl}), 95.9 (HC_{allyl}), 106.6 (C), 129.4 (HC_{Ar}), 130.2 (HC_{Ar}), 130.7 (HC_{Ar}), 134.4 (C_{ipso}), 166.2 (C_{dmf}). MALDI MS: *m/z* 389.1 (M⁺), 353 (M⁺ - Cl - PhCHCH₂).

[Ru(Cp*Cl)(CH₃CCN)(η³-CH₂-CH-CHPh)](PF₆) (**2c**). *tert*-Butylcyanonitrile (2 mL) was added to an oven-dried Schlenk containing [RuCp*Cl(CH₃CN)(η³-CH₂-CH-CH₂)](PF₆), **2a** (60 mg, 0.104 mmol). The reaction mixture was stirred for 2 h, after which the solution was slowly concentrated under vacuum, 58 mg (91%). The resulting crude was washed with CH₂Cl₂/diethyl ether, affording an orange solid, which was filtrated and dried under vacuum. A dichloromethane solution of this solid was then layered with diethyl ether and stored at RT during 16 h, affording bright orange crystals of **2c**, suitable for X-ray diffraction. ¹H NMR (CD₂Cl₂, 298 K, 500 MHz): δ 1.18 (9H), 1.72 (15H), 2.76 (1H, *J* 9.5 Hz), 4.49 (1H, *J* 6.5 Hz), 4.56 (1H, *J* 11.0 Hz), 5.94 (1H, *J* 11.0, 9.5, 6.5 Hz), 7.48–7.54 (4ArH), 7.62 (1ArH). ¹³C NMR (CD₂Cl₂, 298 K, 500 MHz): δ 9.8 (CH₃), 27.6 (CH₃), 68.2 (H₂C_{allyl}), 91.2 (HC_{allyl}), 94.3 (HC_{allyl}), 106.7 (C), 129.5 (C_{Ar}), 129.9 (C_{Ar}), 131.3 (C_{Ar}), 135.1 (C_{ipso}), 137.5 (C_{nitrile}). Anal. Calcd for C₂₄H₃₃ClF₆NPRu: C 46.72, H 5.39, N 2.27. Found: C 46.48, H 5.48, N 2.38. ESI-MS: *m/z* 427.1 (M⁺), 389.1 (M⁺ - (CH₃)₃CCN), 272.0 (M⁺ - (CH₃)₃-CCN - PhCHCH₂).

Accidental Preparation of [RuCpCl₂]₂. [RuCp(CH₃CN)₃](PF₆)-(**5**) (50 mg, 0.115 mmol) was added to a solution of allyl chloride (0.10 mL, 1.22 mmol) dissolved in 4 mL of acetone. The resulting solution was stirred at room temperature for 12 h. Addition of diethyl ether afforded 30.4 mg (95%) of the intended allyl Ru(IV) product. An NMR solution of this Ru(IV) species in acetone-*d*₆ was allowed to stand for 7 days and gave a small crop of orange crystals, which were shown to be the cited decomposition product [RuCpCl₂]₂. [RuCpCl₂(CH₂CHCH₂)] was formed as an orange powder. ¹H NMR (CD₃NO₂, 298 K, 300 MHz): δ 5.73 (5H, Cp),

4.77 (1H, *J* 10.5, 6.0 Hz), 4.21 (1H, *J* 6.0 Hz), 3.91 (2H, *J* 10.5 Hz); (CD₃NO₂, 298 K, 75 MHz): δ 101.83 (CH), 96.21 (C), 67.48 (CH₂). Anal. Calcd for C₈H₁₀Cl₂Ru: C 34.55; H 3.62. Found: C 34.63; H 3.68. ESI-MS: *m/z* 301.0 (RuCl(CH₃OH)₅), 197.2 (RuCp-(CH₃OH)), 139.2 (RuCl).

Acknowledgment. P.S.P. thanks the Swiss National Science Foundation, the “Bundesamt für Bildung und Wissenschaft”, and the ETHZ for financial support. A.A. thanks MURST for a grant (PRIN 2004). I.F. thanks the Junta de Andalucía for a research contract. We also thank Johnson Matthey for the loan of precious metals. The support and sponsorship arranged by

COST Action D24 “Sustainable Chemical Processes: Stereoselective Transition Metal-Catalysed Reactions” is also kindly acknowledged.

Supporting Information Available: Experimental details and a full listing of crystallographic data, including tables of positional and isotropic equivalent displacement parameters, anisotropic displacement parameters, calculated positions of the hydrogen atoms, bond distances, bond angles, and torsional angles for compounds **2b**, **2c**, and **5**. This material is available free of charge via the Internet at <http://pubs.acs.org>.

OM060448U